Title

Visual Stimulation Switches the Polarity of Excitatory Input to Starburst Amacrine Cells

Journal

Neuron, 83(5)

ISSN

0896-6273

Authors

Vlasits, Anna L
Bos, Rémi
Morrie, Ryan D
et al.

Publication Date

2014-09-01

DOI

10.1016/j.neuron.2014.07.037

Peer reviewed

CellPress

Neuron
Article

Visual Stimulation Switches the Polarity of Excitatory Input to Starburst Amacrine Cells

Anna L. Vlasits,[1] Rémi Bos,[2] Ryan D. Morrie,[2] Cécile Fortuny,[3] John G. Flannery,[1,2,3] Marla B. Feller,[1,2,5,*] and Michal Rivlin-Etzion[4,5,*]
[1]Helen Wills Neuroscience Institute
[2]Department of Molecular & Cell Biology
[3]Vision Science Graduate Program
University of California, Berkeley, Berkeley, CA 94720, USA
[4]Department of Neurobiology, Weizmann Institute of Science, Rehovot, 76100, Israel
[5]Co-senior author
*Correspondence: mfeller@berkeley.edu (M.B.F.), michal.rivlin@weizmann.ac.il (M.R.-E.)
http://dx.doi.org/10.1016/j.neuron.2014.07.037

SUMMARY

Direction-selective ganglion cells (DSGCs) are tuned to motion in one direction. Starburst amacrine cells (SACs) are thought to mediate this direction selectivity through precise anatomical wiring to DSGCs. Nevertheless, we previously found that visual adaptation can reverse DSGCs's directional tuning, overcoming the circuit anatomy. Here we explore the role of SACs in the generation and adaptation of direction selectivity. First, using pharmacogenetics and two-photon calcium imaging, we validate that SACs are necessary for direction selectivity. Next, we demonstrate that exposure to an adaptive stimulus dramatically alters SACs' synaptic inputs. Specifically, after visual adaptation, On-SACs lose their excitatory input during light onset but gain an excitatory input during light offset. Our data suggest that visual stimulation alters the interactions between rod- and cone-mediated inputs that converge on the terminals of On-cone BCs. These results demonstrate how the sensory environment can modify computations performed by anatomically defined neuronal circuits.

INTRODUCTION

The retina is a highly organized set of circuits with well-defined cell types and patterns of connections (Masland, 2012). At the same time, the retina is known for its ability to adjust its sensitivity to ambient light levels (Enroth-Cugell and Shapley, 1973; Farrow et al., 2013; Grimes et al., 2014; Ke et al., 2014; Rieke and Rudd, 2009), stimulus contrast (Ke et al., 2014; Manookin and Demb, 2006; Nikolaev et al., 2013), and motion (Olveczky et al., 2007). These adjustments are accomplished through diverse circuit-level mechanisms, which change the roles and receptive fields of individual cells according to the visual environment. Recently, several examples of changes in receptive fields of cells involved in basic computations have been described, including the preferred direction of image motion (Münch et al., 2009; Rivlin-Etzion et al., 2012) and polarity (whether the cell responses to increases or decreases in light intensity) (Gao et al., 2013; Geffen et al., 2007). These adaptations are counter to the retina's well-defined anatomical wiring and suggest that circuit perturbations can dramatically change the computations performed by these neurons.

Previously, we have shown that On-Off direction-selective retinal ganglion cells (DSGCs) reverse their directional preference after visual stimulation with drifting gratings (Rivlin-Etzion et al., 2012). Here we study the effect of the same visual stimulation (referred to as "repetitive stimulation") on starburst amacrine cells (SACs), inhibitory interneurons that are responsible for mediating the direction-selective receptive field of DSGCs (Fried et al., 2002; Lee et al., 2010; Wei et al., 2011). There are two populations of SACs. On-SACs, whose somas reside in the ganglion cell layer and whose processes stratify in the On sublamina of the inner plexiform layer, receive inputs from the On-cone bipolar cells (BCs). Off-SACs, whose somas are located in the inner-nuclear layer and whose processes stratify in the Off sublamina of the inner plexiform layer, receive inputs from Off-cone BCs. Surprisingly, we show that after visual stimulation, excitatory inputs to both classes of cells switch their polarity, resulting in On-SACs responding to decreases in light intensity and Off-SACs responding to increases in light intensity. This polarity switch does not rely upon inhibitory surround circuits in the inner retina; rather, the switch originates presynaptic to BCs via surround circuits in the outer retina. Our results show that visual responses of multiple retinal cell types can vary dramatically within the confines of their strict anatomical wiring.

RESULTS

Reversible Inactivation of SACs Abolishes Direction Selectivity

Previous work demonstrating that SACs are necessary for the computation of direction selectivity used an immunotoxin to kill SACs over the course of days (Amthor et al., 2002; Yoshida et al., 2001), an irreversible perturbation of the circuit. To test unambiguously whether SAC activity is required for generating direction-selective responses, we reversibly inhibited SACs using pharmacogenetics by expressing a chimeric ligand-gated

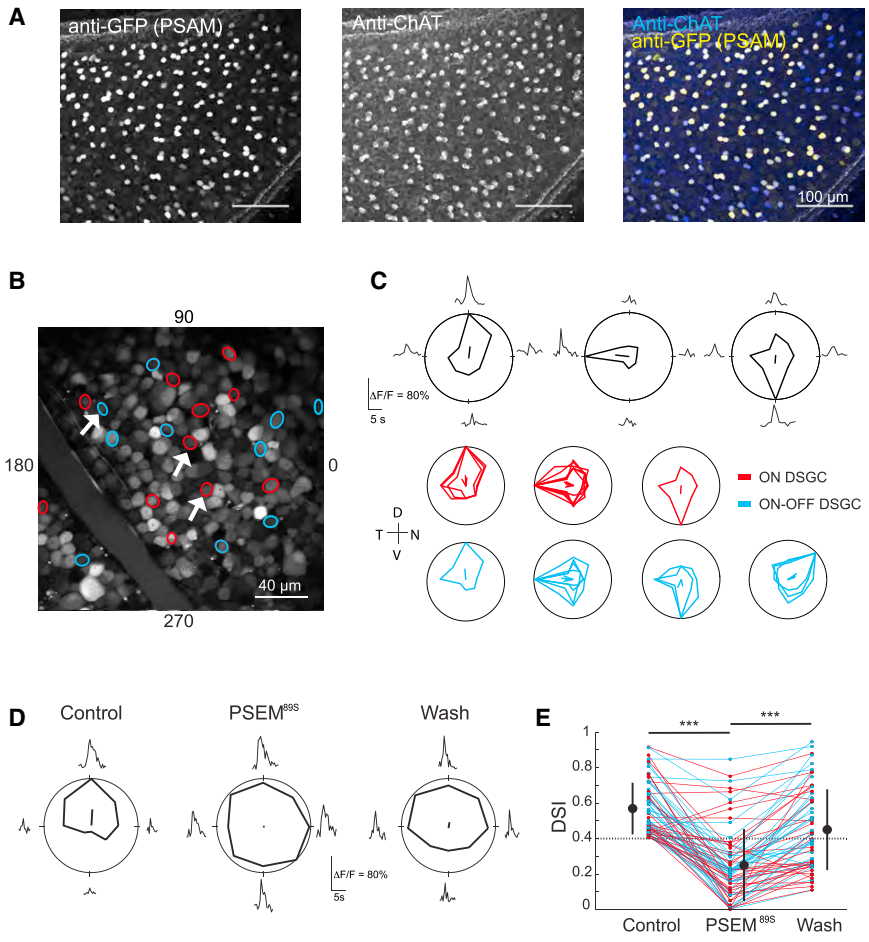

Figure 1. Reversible Inactivation of SACs Abolishes Direction Selectivity

(A) Fluorescence projections of confocal images of the ganglion cell layer of a *ChAT-Cre* mouse retina injected with AAV2-PSAM^{L141F,Y115F}-GlyR-IRES-GFP. Immunostain is for GFP (coexpresses with PSAM, left) and choline acetyltransferase (ChAT), a marker for SACs (middle). GFP-positive cells are also ChAT immunoreactive (right).

(B) Two-photon fluorescence image of the ganglion cell layer of a retina expressing PSAM that has been electroporated with cell-impermeant Oregon green 488 BAPTA-1. Circles are cells identified as DSGCs, color-coded by response type (red: On DSGCs, blue: On-Off DSGCs). White arrows correspond to the individual tuning curves in (C).

(C) Top: examples of average calcium responses ($\Delta F/F_0$) and tuning curves of three DSGCs (white arrows in B) in response to a UV bar moving in eight different directions. The solid lines inside the polar plots indicate the vector-summed response corresponding to the preferred direction. Bottom: tuning curves for all of the DSGCs imaged in (B). Each tuning curve is normalized to the maximum response for each cell. Color codes as in (B). Axes of the retina are indicated to the left of the plots; D, dorsal; N, nasal; T, temporal; V, ventral.

(D) Example tuning curve of a DSGC before (control), during (PSEM^{89S}), and after (Wash) the addition of PSEM^{89S}.

(E) Effect of PSEM^{89S} on the direction-selective index (DSI) of DSGCs (n = 68 cells) in five retinas. Large circles indicate group means, error bars represent SD, dotted line indicates the threshold DSI for defining a cell as a DSGC (DSI > 0.4). *** indicates $p < 0.001$, Tukey post hoc test. Color codes are as in (B).

See also Figure S1.

chloride channel, PSAM^{L141F,Y115F}-GlyR (PSAM; Magnus et al., 2011) in SACs (Figure 1A). This was achieved by intravitrial injection into *Chat-cre* mice of a 7m8-AAV2 virus (Dalkara et al., 2012, 2013) carrying a *flex-PSAM-IRES-GFP* gene. Application of the synthetic ligand PSEM^{89S} to the retina reversibly opened the PSAM chloride channels, which significantly reduced the mean input resistance of On-SACs (297 ± 84.6 MΩ before addition of PSEM^{89S} to 164 ± 66.4 MΩ in PSEM^{89S}, n = 6 cells, $p < 0.05$).

To assess the effect of activating PSAM on direction selectivity, we loaded retinas expressing PSAM with the calcium dye Oregon green 488 Bapta-1 via electroporation and characterized responses to drifting bars using two-photon calcium imaging (Briggman and Euler, 2011; Briggman et al., 2011; Yonehara et al., 2013). Both On-Off DSGCs and On-DSGCs were detected (Figures 1B and 1C). After application of PSEM^{89S}, the vast majority of DSGCs lost their directional tuning, responding equally to motion in all directions (DSI for control: 0.57 ± 0.15; for PSEM: 0.25 ± 0.20; for Wash: 0.45 ± 0.22; n = 68 cells from 5 retinas; one-way ANOVA, $p < 0.001$; Tukey post hoc for Control versus PSEM, $p < 0.001$; for PSEM versus Wash, $p < 0.001$; Figures 1D and 1E), consistent with a loss of direction-selective inhibition from SACs. Addition of PSEM^{89S} to wild-type retinas, which did not express PSAM, resulted in no change in the DSI of DSGCs (Figure S1 available online, DSI for control: 0.57 ± 0.14; for PSEM: 0.56 ± 0.15, n = 46 cells from 4 retinas; paired t test $p = 0.7$), indicating that there were no off-target effects of PSEM^{89S}. These data demonstrate the requisite role of SACs in the direction-selective computation and demonstrate that the reduction in SAC excitability using PSAM is sufficient to prevent their participation in the direction-selective circuit.

Starburst Amacrine Cells Switch Their Polarity as A Result of Visual Stimulation

Previously, we found that visual adaptation using repetitive stimulation induced a reversal of the directional tuning of DSGCs. In addition, repetitive stimulation induced changes in the synaptic inputs to DSGCs, most notably the inhibitory inputs (Rivlin-Etzion et al., 2012), suggesting that the repetitive stimulation might alter the light responses of SACs. We performed two-photon targeted whole-cell voltage-clamp recordings from transgenically labeled SACs (Rivlin-Etzion et al., 2012; Wei et al., 2010; Figure 2A) to characterize the effect of repetitive stimulation on the response to increases and decreases in illumination using a 2 s stationary white spot projected onto the retina. Initially, our recordings from On-SACs were restricted to the dorsal half of the retina where our visual stimulus would robustly activate the cones sensitive to

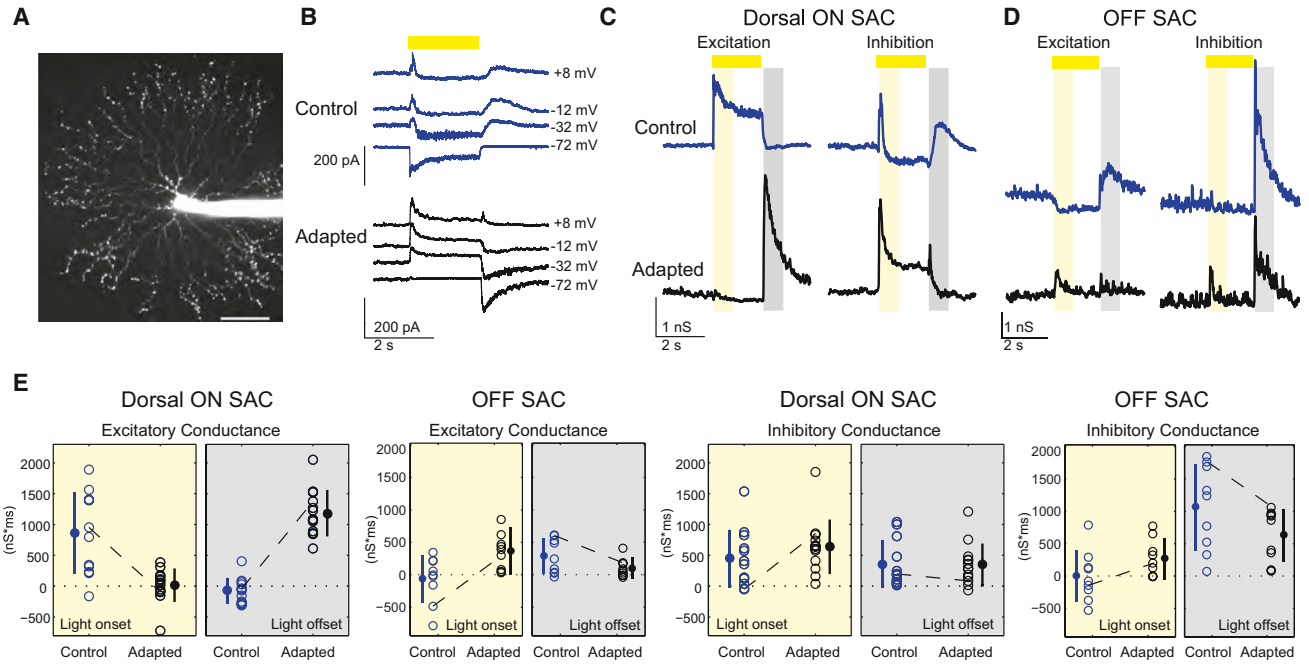

Figure 2. SACs Switch Their Polarity as a Result of Visual Stimulation

Blue data, controls (before adaptation); black data, adapted cells. Light stimulation is indicated by the yellow bar.

(A) Projection of fluorescence image of an Off-SAC filled with Alexa Fluor 594; scale, 50 μm.

(B) Synaptic currents onto a dorsal On-SAC at different holding potentials in response to a 2 s light spot (225 μm diameter) before (top) and after (bottom) adaptation. Traces are averages of five sweeps.

(C and D) Excitatory and inhibitory conductances from a dorsal On-SAC (C) and an Off-SAC (D) were evaluated at 10 ms intervals based on the I-V relations in response to a 2 s white spot stimulus. The On-SAC conductances correspond to the current measurements shown in (B). The time periods for calculating the integrated conductances (see E below) are indicated by the yellow rectangle for light onset (50–850 ms after light onset) and by the gray rectangle for light offset (100–900 ms after light offset).

(E) The integrated excitatory and inhibitory conductances during light onset and light offset for dorsal On-SACs and all Off-SACs before and after adaptation. Empty circles are conductances in individual cells. Dashed lines represent the example cells shown in (C) and (D). Mean values are represented by the filled circles, error bars indicate SD.

See also Figure S3.

green light (Breuninger et al., 2011; Wang et al., 2011). Currents were measured at four different holding potentials (Figure 2B, blue), allowing us to perform conductance analysis to isolate the excitatory inputs from the inhibitory inputs (Figure 2C, blue; Taylor and Vaney, 2002; see Supplemental Experimental Procedures). We then exposed the retina to the repetitive stimulation previously shown to reverse the direction preference of DSGCs (Rivlin-Etzion et al., 2012) and repeated the light spot stimulation and conductance analysis (Figures 2B and 2C, black).

Before repetitive stimulation, On-SACs exhibited a large excitatory conductance at light onset but not at light offset (Figures 2B and 2C, blue). After repetitive stimulation, many On-SACs lost their excitatory input at light onset and, surprisingly, gained an excitatory input at light offset, thereby switching their polarity (Figures 2B and 2C, black). In contrast, the inhibitory conductance onto On-SACs was observed at light onset as well as at light offset both before and after repetitive stimulation, indicating that the basic organization of inhibition did not change. We refer to the state after repetitive stimulation as "adapted."

To compare control and adapted populations, we quantified the overall conductances of each SAC at light onset and light offset (Figure 2E). The population analysis demonstrates that adapted On-SACs in the dorsal half of the retina had a reduced excitatory conductance at light onset (863 ± 664 nS × ms in controls, n = 12; 16 ± 272 nS × ms in adapted cells, n = 13; $p < 0.01$; Figure 2E) and gained an excitatory conductance at light offset (−70 ± 206 nS × ms in controls; 1,184 ± 377 nS × ms in adapted cells; $p < 0.01$). Inhibitory conductance onto adapted On-SACs did not significantly change ($p = 0.17$ and $p = 0.68$ for light onset and light offset, respectively). To verify that changes in conductance of adapted On-SACs did not emerge as a result of prolonged whole-cell recordings, we presented the adapted stimulus to a subset of cells before recording from them (n = 4/13 On-SACs; see Table S1 for details on sample sizes for this and subsequent experiments).

We executed the same protocol on Off-SACs, which also exhibited a polarity switch, increasing their excitatory conductance in response to light onset (−70 ± 361 nS × ms in controls; 358 ± 276 nS × ms in adapted cells; $p < 0.05$; Figures 2D and 2E; note: Off-SACs were recorded from both dorsal and ventral regions of the retina). The excitatory conductance of adapted Off-SACs in response to light offset was not changed significantly

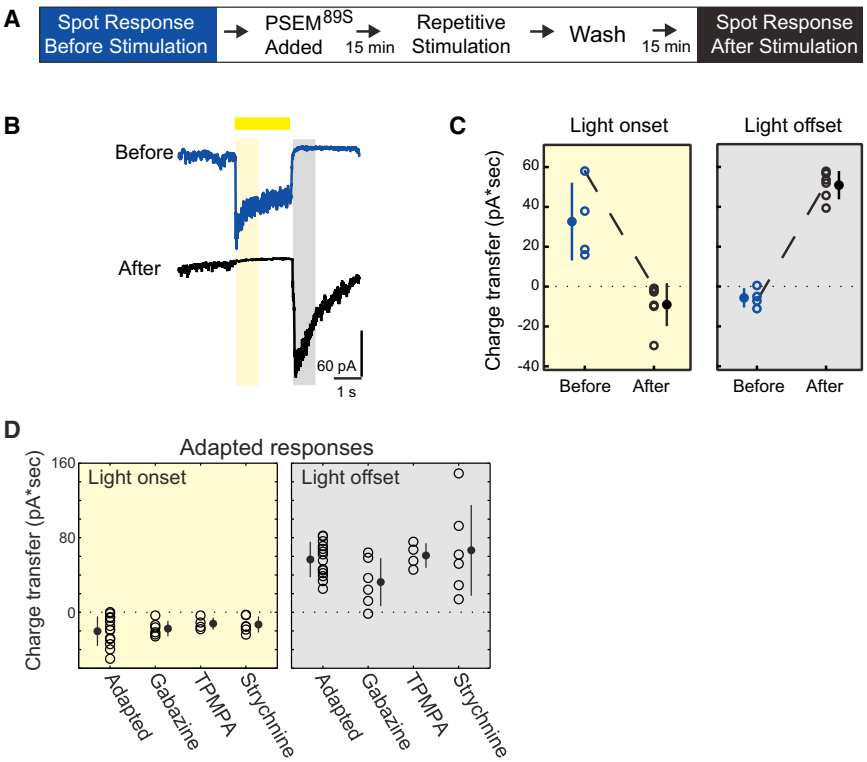

Figure 3. Polarity Switch Occurs Independent of SAC Activity and Inhibitory Circuits

(A) Protocol for assessing SAC adaptation in the presence of PSEM^{89S}. PSEM^{89S} was present during the repetitive stimulation but not while measuring the response to light spot stimuli before and after stimulation.

(B) Example of voltage-clamp recording (average of five sweeps) from PSAM-expressing On-SAC held at −72 mV during light spot stimuli presented before and after the protocol outlined in (A). The time periods for calculating the charge transfer are indicated by the yellow rectangle for light onset (50–850 ms after light onset) and by the gray rectangle for light offset (100–900 ms after light offset).

(C) Charge transfer (averaged over five sweeps) of the excitatory current during light onset and light offset as specified by the yellow and gray boxes in (B) for On-SACs before and after stimulation in the presence of PSEM^{89S}. The dotted line is the cell in (B).

(D) The excitatory charge transfer during light onset (yellow) and light offset (gray) in individual adapted On-SACs in control solution (Adapted) and after application of 5 μM gabazine, 50 μM TPMPA, or 1 μM strychnine.

For (C and D) Empty circles indicate individual cells, solid circles represent mean, error bars indicate SD.

See also Figure S2.

(p = 0.14). After repetitive stimulation, inhibition onto Off-SACs was also not changed significantly (p = 0.09 and p = 0.22 for light onset and light offset, respectively).

Polarity Switch Occurs Independent of SAC Activity and Inhibitory Circuits

The above experiments demonstrate that the excitatory inputs to SACs are dramatically altered after repetitive stimulation, indicating that the site of modulation is the BC terminal presynaptic to SACs. GABA-A and GABA-C receptors are localized to the terminals of On-cone BCs and therefore can provide a powerful inhibition of glutamate release (Sagdullaev et al., 2006). It has been postulated that the asymmetric release of glutamate associated with direction selectivity in DSGCs is due to feedback inhibition from SACs onto the terminals of On-cone BCs (Vaney et al., 2012; Wei and Feller, 2011) (but see recent findings indicating glutamate release is not modulated by motion stimulation [Park et al., 2014; Yonehara et al., 2013]).

To test whether the polarity switch is due to a change in SACs's feedback inhibition onto BCs, we reversibly inhibited SACs during repetitive stimulation in mice expressing PSAM in SACs by adding PSEM^{89S} only during the repetitive stimulation (Figure 3A). We found that dorsal On-SACs still switched their polarity when the SAC activity is reduced by PSEM^{89S} during the repetitive stimulus (Figures 3B and 3C); On-SACs lose their excitatory current at light onset (control, 32.6 ± 19.5 pA × s; stimulated, −9.0 ± 10.8 pA × s) and gain an excitatory current at light offset after repetitive stimulation (control, −5.7 ± 4.9 pA × s; stimulated, 50.8 ± 7.1 pA × s).

While it is known that GABA-A receptors mediate inhibition between On-SACs, blocking GABA-A signaling before repetitive stimulation did not abolish inhibitory input to On-SACs, suggesting that the combination of inhibitory inputs to these cells is complex (Figure S2). We tested whether acute blockade of inhibition from SACs and other sources could affect the excitatory Off response gained after repetitive stimulation. Addition of either GABA-A or GABA-C receptor blockers (5 μM gabazine and 50 μM TPMPA, respectively) to the solution after repetitive stimulation did not abolish the adapted Off response (Figure 3D; Figure S2), confirming that inhibitory feedback from SACs or any other GABAergic amacrine cell did not mediate the adapted Off response. Another source of modulation of release from BCs terminals is crossover inhibition, which is mediated by both glycinergic and GABAergic amacrine cells (Werblin, 2010). We found that the addition of the glycine receptor antagonist strychnine (1 μM) after repetitive stimulation did not eliminate the Off response charge transfer or conductance in On-SACs (Figure 3D; Figure S2).

Together, these data rule out a role for inner retina inhibitory circuits in the polarity switch in On-SACs, suggesting that the polarity switch is not due to feedback, crossover inhibition, or surround interactions in the inner retina.

Gain of Off Response Requires Cone Activation

How is repetitive stimulation altering the release of glutamate from BCs? Light responses in the mouse retina are mediated by interactions of cone and rod pathways (Grimes et al., 2014; Ke et al., 2014; Münch et al., 2009; Wang et al., 2011) (Figure 4A).

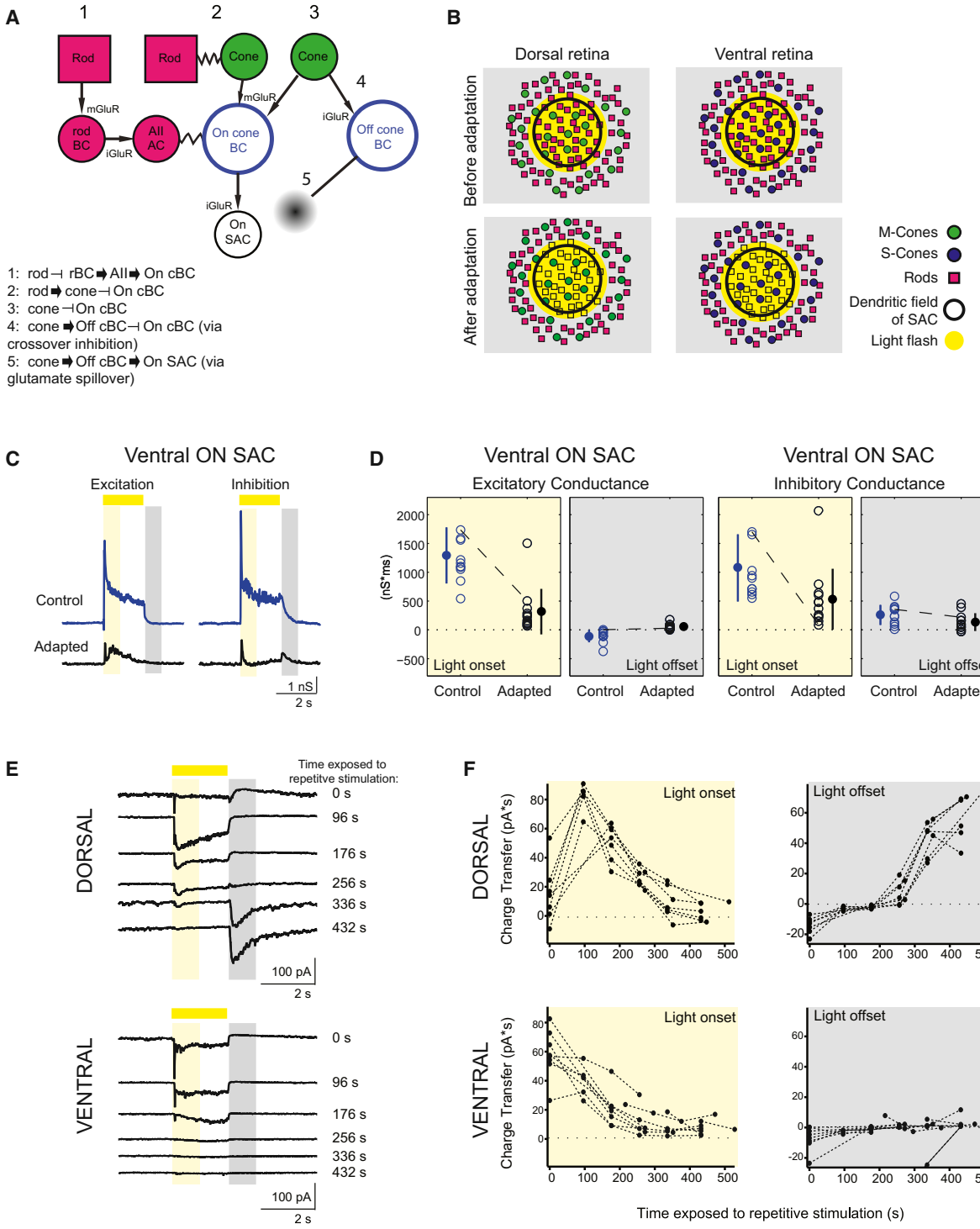

Figure 4. Gain of Off Response Requires Cone Activation

(A) Schematic of potential pathways that could influence signaling in On-SACs.

(B) Schematic of experimental results. Light stimulation with an OLED activated both rods and cones in the dorsal retina and only rods in ventral retina. After repetitive stimulation, rods are no longer responsive to light spots.

(C) Excitatory and inhibitory conductances from a ventral On-SAC. Conventions are as in Figure 2C.

(D) The integrated excitatory and inhibitory conductances during light onset and light offset for ventral On-SACs before and after adaptation. Conventions are as in Figure 2E.

(legend continued on next page)

Hence, the loss of the On response and the appearance of the Off response in On-SACs may result from a change in the interaction between these pathways. To isolate the contributions of rod and cone pathways, we took advantage of the ventral-to-dorsal gradient of cone opsin expression, as cones in the ventral retina are dominated by UV opsins, while those in the dorsal retina are dominated by green opsins (Applebury et al., 2000; Calderone and Jacobs, 1995) (Figure 4B). These experiments were conducted using visual stimuli that did not strongly activate UV opsins (Wang et al., 2011). Thus, to minimize the cone contribution, we monitored the effects of repetitive stimulation on ventral On-SACs. We found that after repetitive stimulation, On-SACs in the ventral half of the retina lost their excitatory input at light onset in a manner similar to On-SACs in dorsal retina (from 1,294 ± 487 nS × ms in controls to 317 ± 395 nS × ms in stimulated cells; $p < 0.01$; quantification of the sustained component of the light response is provided in Figure S3). Conversely, ventral On-SACs did not gain a large Off response after repetitive stimulation, though there was a slight increase in the integrated-conductance (−107 ± 107 nS × ms in controls; 55 ± 48 nS × ms in adapted cells; $p < 0.01$; Figures 4C and 4D). These data indicate that the On response lost after repetitive stimulation is due primarily to a loss of rod-mediated signaling, while the Off response gained after repetitive stimulation occurred uniquely in the dorsal half of the retina, suggesting that strong activation of cones is required for the polarity switch.

One simple explanation for the switch in polarity of the excitatory inputs to On-SACs is that the strong repetitive stimulation has saturated the rod photoreceptors such that they no longer respond to light spots. Indeed, the light levels used during repetitive stimulation can lead to saturation of rods (Wang et al., 2011), which cannot recover since our preparation does not have a pigment epithelium. In this scenario, the Off response gained after repetitive stimulation is mediated by cones; the difference between the effect of repetitive stimulation on dorsal and ventral On-SACs supports this idea.

To further explore the dependence of the Off response on the loss of the On response, we characterized the time course of adaptation by recording the excitatory currents in On-SACs in response to stationary white spots in between bouts of repetitive stimulation. In dorsal On-SACs, exposure to the repetitive stimulus initially led to an increase in excitatory charge transfer followed by a slow loss of the On response after exposure to ~400 s of the repetitive stimulus. In these cells, the excitatory Off response emerged after 250–350 s exposure to the repetitive stimulus and persisted for as long as the recording (Figures 4E and 4F, top). In contrast, in ventral On-SACs we observed a slow loss of the excitatory On response over the course of the recording, but we did not observe an excitatory Off response emerge in these cells (Figures 4E and 4F, bottom). These data indicate that (1) the Off response is mediated by cones and (2) this cone-mediated Off response emerges only in the absence of a robust On response.

On-Cone BCs Mediate Polarity Switch in SACs

To further explore the mechanism that underlies the polarity switch in SACs, we set out to study the source of the Off response gained after repetitive stimulation of dorsal On-SACs. Connectomic reconstructions of the inner retina confirm that On-SACs only receive inputs from On-cone BCs and not from Off-BCs (Helmstaedter et al., 2013) (Figure 4A), and functional glutamate imaging showed limited spillover between On and Off pathways (Borghuis et al., 2013). Before repetitive stimulation, excitatory input onto On-SACs was mediated exclusively via the On pathway, since hyperpolarization of On-cone BCs using the mGluR6 agonist L-AP4 (5 μM; (Slaughter and Miller, 1981)) blocked excitation completely (Figure S4B). Addition of L-AP4 to adapted On-SACs abolished both excitatory and inhibitory inputs in response to light offset (Figure 5A, Figure S4A). These data indicate that the Off response gained after repetitive stimulation originates from the On pathway and not via spillover from the Off pathway (Figure 4A, pathways 4 and 5).

Further evidence that the repetitive stimulation alters the On-pathway is the observation that spontaneous glutamate transmission from On-cone BCs changed after adaptation. Exposure to repetitive stimulation significantly increased excitatory spontaneous activity at light offset, as measured by the variance in the holding current (from 6.77 ± 2.74 pA^2 to 45.43 ± 24.90 pA^2; paired t test: $p < 0.01$; Figures 5B and 5C), indicating that the adapted On-SACs were tonically depolarized in the dark because of tonic glutamate release from On-cone BCs. This elevated level of tonic glutamate release from On-cone BCs onto adapted On-SACs after repetitive stimulation was suppressed by light (Figures 5D and 5E). By hyperpolarizing On-cone BCs with L-AP4, we abolished tonic glutamate transmission in the dark (Figures 5D and 5E). These observations confirm that the Off response observed in On-SACs is mediated by glutamate release from On-cone BCs and suggest that, in the adapted state, On-cone BC terminals are depolarized in the dark and hyperpolarized in the light.

A previous study at cone photoreceptor synapses provides an interesting hypothesis as to how suppression of glutamate release during light stimulation can lead to the generation of an Off response. Cone photoreceptors exhibit buildup of glutamatergic vesicles at the ribbon synapse when the light is on; when the light is turned off, this suppression is relieved, and the excess vesicles that have crowded at the bottom of the ribbon are released (Jackman et al., 2009). This model was based

(E) Voltage-clamp recordings of excitatory currents from dorsal (top) and ventral (bottom) On-SACs (holding potential = −72 mV) in response to a 2 s light spot (225 μm diameter). Spots were presented in between exposing the cells to repetitive stimulation, with the time exposed to repetitive stimulation indicated on the right. Traces are averages of five sweeps. The time periods for calculating the charge transfer are indicated by the yellow rectangle for light onset (50–850 ms after light onset) and by the gray rectangle for light offset (100–900 ms after light offset).

(F) Charge transfer (averaged over five sweeps) of the excitatory current during light onset and light offset for dorsal (top) and ventral (bottom) On-SACs as a function of the amount of time cells were exposed to gratings.

See also Figure S3.

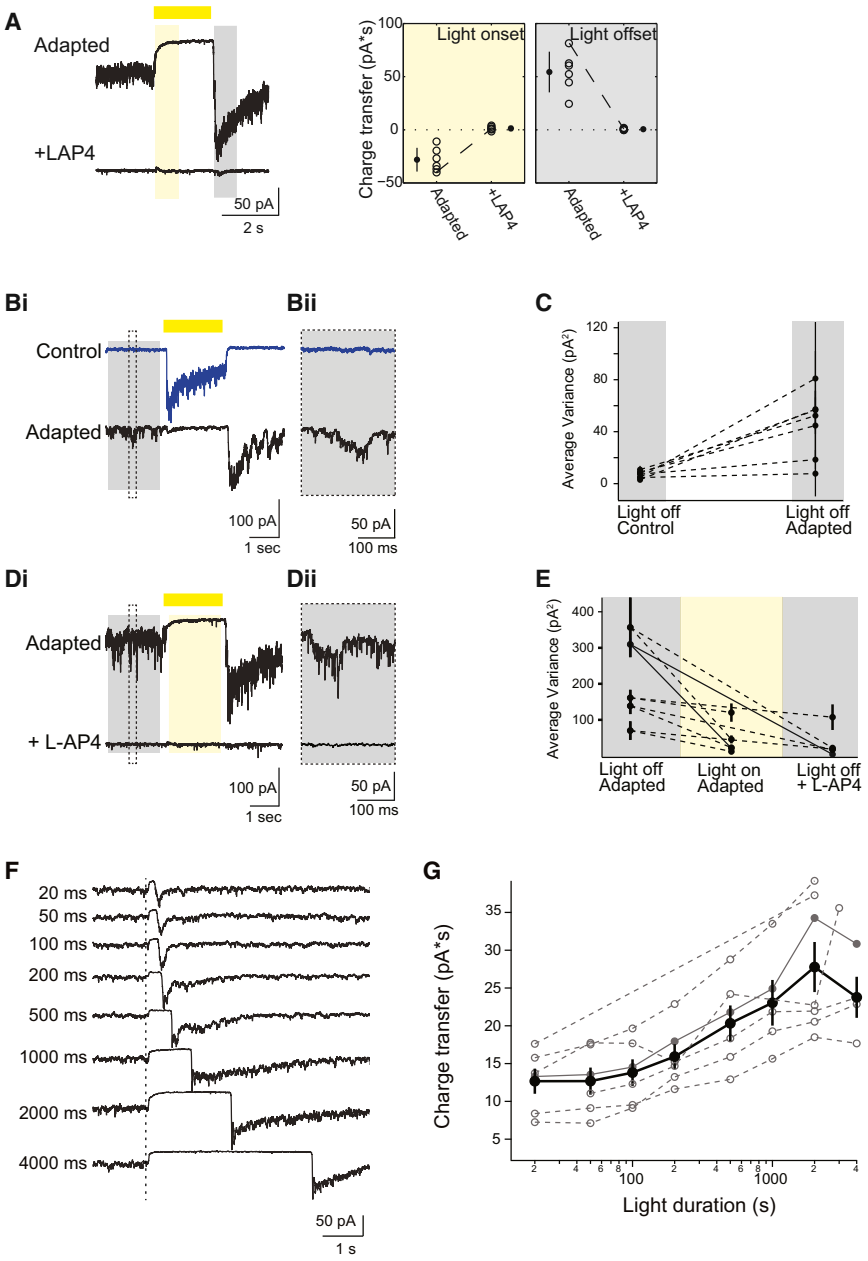

Figure 5. On-Cone BCs Mediate Polarity Switch in SACs

(A) Left: excitatory current in adapted On-SACs in control solution (top) and after application of 5 μM L-AP4 (bottom) (holding potential = −72 mV). Conventions are as in Figure 3B. Right: the excitatory charge transfer at light onset and light offset for adapted On-SACs in control solution and in L-AP4. Conventions are as in Figure 3C.

(Bi and Bii) Individual voltage-clamp sweeps at −72 mV holding potential showing the excitatory current during presentation of a 2 s light flash (yellow bar) in an On-SAC before and after repetitive stimulation. The time period used to measure the variance in the holding current quantified in (C) is represented by the gray box. Dotted line indicates the inset in (Bii) showing the spontaneous activity.

(C) The variance of the excitatory current of On-SACs (n = 6 cells) during the 1,800 ms "light off" period (gray box in Bi). For each cell, the average of the variance from five sweeps is plotted (black dots) with the SD.

(Di and Dii) Individual voltage-clamp sweeps at −72 mV holding potential showing the excitatory current in an adapted On-SAC during presentation of a 2 s light flash (yellow bar) in control solution (above) and after adding 5 μM L-AP4 (below). Dotted box is the timing of the inset in (Dii) showing the spontaneous activity, the gray rectangle is the time period used for "light off" analysis in (E), and yellow rectangle is the time period used for "light on" analysis in (E).

(E) The variance of the excitatory current in adapted On-SACs (n = 5 cells) during 1,800 ms "light off" and "light on" periods (gray and yellow rectangles in Di, respectably). For each cell, the average of the variance from five sweeps is plotted (black dots) with the standard deviation. Solid lines represent the variance for the example cell in (D).

(F) Voltage-clamp recordings (holding potential = −72 mV) from an On-SAC. Dotted line is the time of light onset. Duration of the light flash is indicated by the time to the left of traces. Traces are averages of five sweeps.

(G) Excitatory charge transfer during the 400 ms after the time of the maximum current as a function of light flash duration plotted on a semi-log scale. Open gray circles, individual cells. Closed gray circles, example cell shown in (F). Black circles, average across cells. Error bars represent SEM. See also Figure S4.

in part on the observation that the magnitude of the Off-response was correlated with the length of light-mediated suppression of glutamate release (Jackman et al., 2009). Similarly, we found that the Off excitatory charge transfer after repetitive stimulation increased with increasing stimulus duration, with the effect saturating at longer durations (Figures 5F and 5G). This supports the idea that the excitatory Off response in adapted On-SACs arises because of suppression of release and accumulation of glutamatergic vesicles during light stimulation at a ribbon synapses; however, it does not distinguish whether suppression occurs at BC or at photoreceptor terminals.

Polarity Switch Depends on Changing Contribution of Rod Circuit

The above experiments indicate that the Off response gained after repetitive stimulation is mediated by glutamate release from On-cone bipolar terminals. As noted previously, the Off response gained after repetitive stimulation was observed in dorsal but not ventral retina, indicating that the response originates from cones (Figures 2 and 4). Cones can influence the membrane potential of On-cone BCs terminals either via their direct, sign-inverting glutamatergic synapse with On-cone BCs (Figure 4A, pathway 3) or through signaling to rods via Cx36-mediated gap junction coupling between rods and cones (Deans et al., 2002) (Figure 4A,

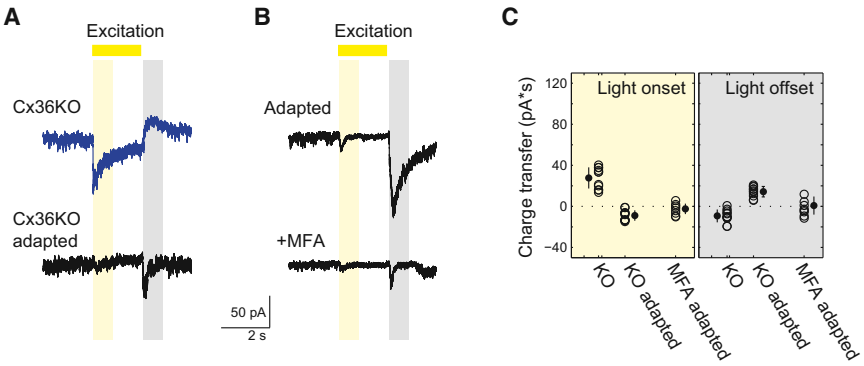

Figure 6. Polarity Switch Depends on Changing Contribution of Rod Circuit

(A) Voltage-clamp recordings (holding potential = −72 mV) from an On-SAC from a *Cx36* KO mouse in control conditions (top) and after adaptation (bottom).

(B) Voltage-clamp recordings (holding potential = −72 mV) from an On-SAC after adaption in control conditions (top) and in the presence of the gap junction antagonist MFA (bottom).

(C) The excitatory charge transfer during light onset (yellow) and light offset (gray) in individual On-SACs (circles) from *Cx36* KO retinas before (KO) and after (KO adapted) adaptation and from WT retinas after adaptation in the presence of 100 μM meclofenamic acid (MFA adapted). Error bars represent SD.

See also Figure S5.

pathway 2). This second pathway through rods feeds forward to On-cone BCs via rod BCs that form excitatory synapse onto AII amacrine cells, which in turn are gap junction coupled to On-cone BCs, also via Cx36 gap junctions (Deans et al., 2002; Grimes et al., 2014) (Figure 4A, pathway 1).

To test whether cone signaling through the rod pathway (Figure 4A, pathways 1 and 2) might mediate the change in On-cone BC glutamate release, we repeated the experiment in *connexin-36* knockout (*Cx36* KO) mice. Before repetitive stimulation, *Cx36* KO mice exhibited a smaller, though not significant, excitatory input at light onset compared to WT (50.7 ± 35.9 in WT mice; 27.7 ± 10.3 pA × s in KO mice; $p = 0.13$); after repetitive stimulation, they have a significantly smaller excitatory input at light offset compared to WT (65.5 ± 17.4 in WT mice; 14.3 ± 5.1 pA × s in KO mice; $p < 0.01$) (Figure 6A; Figure S5). These findings suggest that through gap junction coupling, the rod pathway contributes to release from On-cone BCs before and after repetitive stimulation and that the rod pathway not only drives excitatory input onto On-SACs but also modulates the amplitude of the Off response obtained after adaptation. This is surprising given that repetitive stimulation reduced the rod-mediated On response in ventral retina (Figure 4) and indicates that the rod pathway may contribute via inhibitory feedback from cones (this hypothesis is explored further in the Discussion and Figure 7).

Importantly, while excitation was reduced after repetitive stimulation, On-SACs in *Cx36* KO mice still exhibited loss of the On response and gain of the Off response after repetitive stimulation (Figures 6A and 6C; Figure S5; from 27.7 ± 10.3 in control to −8.9 ± 5.1 pA × s in adapted cells for light onset; $p < 0.01$; and from −9.3 ± 6.3 in control to 14.3 ± 5.1 pA × s in stimulated cell for light offset; $p < 0.01$). This suggests that while the rod pathway modulates the amplitude of the Off response after repetitive stimulation, the polarity switch still takes place in the *Cx36* KO. Because the AII amacrine cell to On-cone BC electrical synapse is composed of heterologous connexins containing both Cx36 and Cx45 (Dedek et al., 2006), we utilized meclofenamic acid (MFA; 100 μM), a general gap junction blocker, to more completely block gap junction in the rod circuit. In the presence of MFA, the excitatory charge transfer and conductance after repetitive stimulation at light offset was abolished (Figures 6B, 6C, and S5). Note that, before repetitive stimulation, addition of 100 μM MFA led to a sharp decrease in excitatory conductance onto On-SACs, consistent with our recordings from the *Cx36* KO (Figure S5).

Together, these data indicate that (1) rod-mediated signals comprise a significant component of the On response observed in On-SACs; (2) rod-mediated On signals are lost after adaptation; and (3) the generation of the Off-response after repetitive stimulation occurs independently of rod transduction. We propose that the Off response is generated in the BC surround by a cone-mediated depolarization of rods (Figure 7), a pathway that becomes active only after loss of the rod-mediated responses. A full description of this model is presented in the Discussion.

SAC Polarity Switch Could Mediate Reversed Tuning of DSGCs

What are the circuit implications for a polarity switch in SACs? Because inhibition from SACs is necessary for the tuning of DSGCs (Figure 1), we hypothesized that the polarity switch in SACs after repetitive stimulation would shift the phase of GABA release relative to a drifting gratings stimulation and that this phase shift contributes to the reversal of the preferred direction of DSGCs. To test this hypothesis, we created a simulation. We assumed that since there are subtypes of BCs that innervate exclusively SACs but not DSGCs (Helmstaedter et al., 2013), the timing of excitatory input onto DSGCs is not shifted in a similar manner. We simulated the changes in the membrane potential of a DSGC and the spiking activity generated by these changes in response to drifting gratings in the preferred direction (PD) and null direction (ND) (Figure 8). For simplification, the simulation included responses mediated only by the On pathway. Excitatory and inhibitory conductances onto DSGCs were simulated as rectified sinusoids. The excitatory conductance onto DSGCs was similar during both PD and ND drifting grating stimulation, while the inhibitory conductance mediated by On-SACs was continuously shifted in phase relative to excitatory conductance (Park et al., 2014). Prior to repetitive stimulation, the inhibitory conductance in response to ND stimulation was coincident with the excitatory conductance, thereby preventing depolarization in the DSGC. In response to PD stimulation, the inhibitory conductance was delayed relative to excitation, allowing the

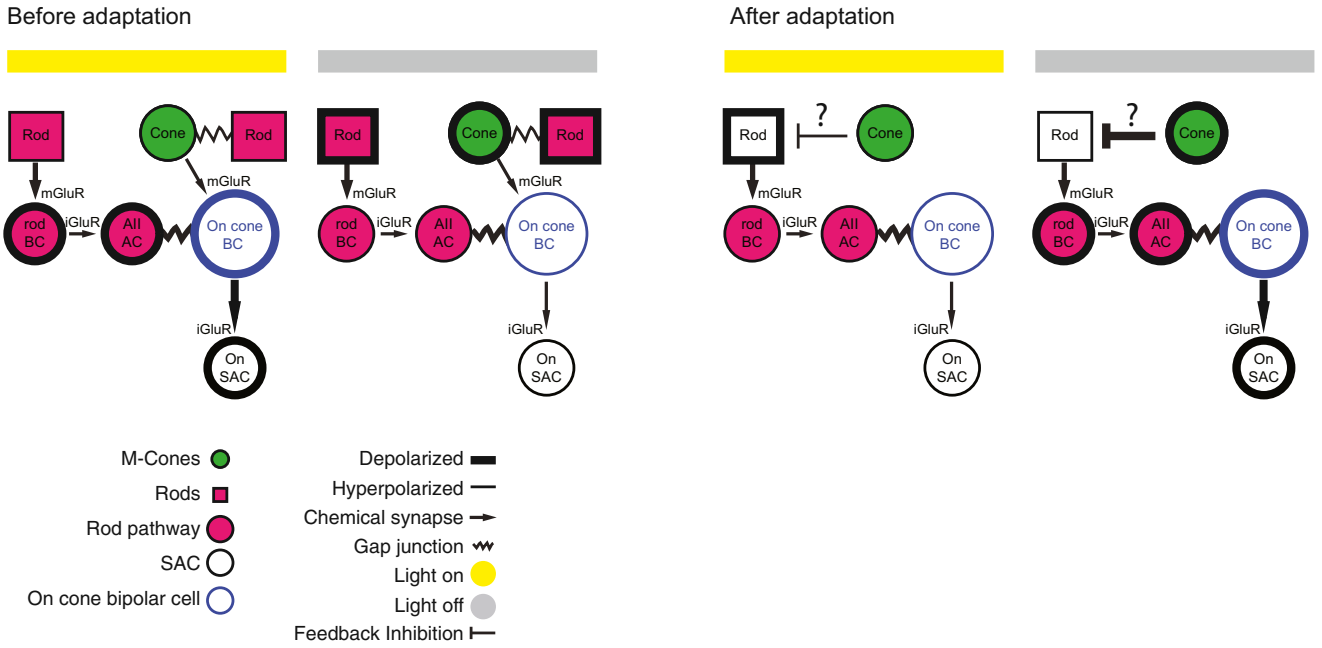

Figure 7. Proposed Model of Polarity Switch in the Retinal Circuit
Schematic of circuit that mediates light responses prior to and after adaptation. Details are provided in the Discussion.
See also Figure S6.

DSGC to depolarize. We calculated the weighted difference between the spiking in response to PD versus ND to determine the direction-selective index (DSI, see Experimental Procedures). Before repetitive stimulation, we calculated DSI = 1. We defined this condition as phase shift = 0 (Figure 8A, left).

By examining DSI as a function of the phase shift, we found that DSI values were negative for a range of phases around half-a-cycle shift (π), indicating that the DSGC has reversed its directional preference for a wide range of phase shifts (Figure 8B). The excitatory and inhibitory conductances onto the DSGC that lead to the minimal DSI value are shown in Figure 8A, right. Here, the inhibitory conductance was half-a-cycle shifted in time relative to excitation, resulting in more depolarization in response to ND stimulation. The same temporal shift caused the inhibitory conductance to be synchronous with excitation in response to PD stimulation. This led to a reduced depolarization in response to PD stimulation. Such a phase shift is expected if the SACs have a polarity switch in their phase, i.e., if On-SACs respond to a decrease in light intensity rather than an increase. Furthermore, asymmetric wiring of SACs creates a smaller PD inhibitory conductance, but if phase shifted as in the model, this smaller conductance would be effective enough to shunt the excitatory current on the DSGC (see Figures 3C and 3D of Rivlin-Etzion et al., 2012). Thus, a polarity switch in SACs postulates a potential contribution for reversed tuning of DSGCs.

DISCUSSION

We demonstrated that silencing SACs in a reversible manner transiently eliminates direction-selective responses in DSGCs, indicating a requisite role for SAC signaling in the computation of direction selectivity. Furthermore, presenting the retina with a repetitive visual stimulus consisting of drifting gratings, a protocol known to reverse the direction selectivity of DSGCs, caused the excitatory synaptic input to SACs to switch its polarity. The switch occurs independently of GABA-A, GABA-C, and glycine signaling. Rather, our data suggest that repetitive stimulation leads to a reduction in the On response followed by an increase in cone-mediated signaling that occurs at light offset and leads to an Off response in On-cone BCs. As an example of how these changes in signaling in the outer retina can profoundly alter the response properties in the inner retina, we use modeling to demonstrate how this flip in polarity of SACs may contribute to the reversal in the directional tuning of DSGCs (Rivlin-Etzion et al., 2012).

Mechanism Involves Changes in Circuits in the Outer Retina

The polarity switch in On-SACs is comprised of two components—the loss of the On response and the gain of an Off response. The former occurred in all regions of the retina, while the latter occurred exclusively in the dorsal half of the retina. Two key facts allowed us to understand this difference between dorsal and ventral regions. First, there is a gradient of cone opsin expression in the mouse retina, with M-cones dominating in the dorsal retina and S-cones dominating in the ventral retina (Breuninger et al., 2011; Ekesten and Gouras, 2005; Wang et al., 2011). Second, our visual stimuli preferentially activate M-cones and rods but not S-cones (Wang et al., 2011). This suggests that the gain of the Off response, which only occurred in the dorsal

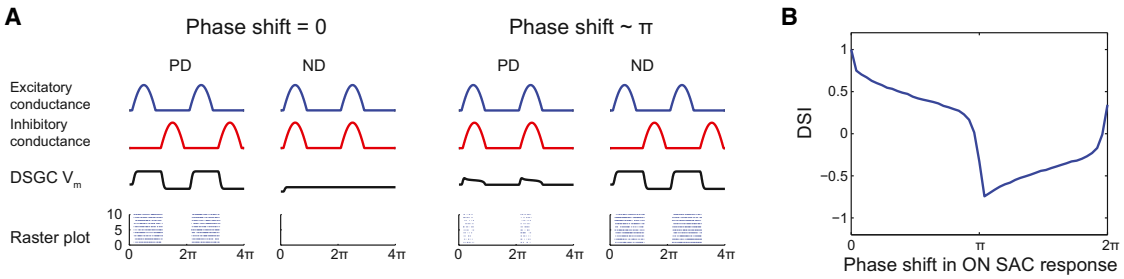

Figure 8. SAC Polarity Switch Could Mediate Reversed Tuning of DSGCs

(A) Excitatory conductance from On-cone BCs (blue), inhibitory conductance from On-SACs (red), and resulting changes in membrane potential in DSGC (V_m, black) in response to drifting grating in PD and ND (response to two phases of grating are shown). Bottom: raster plots depict spiking activity in DSGC randomly generated based on membrane potential values in ten repetitions of the stimulus. The examples on left and right represent the phase shifts that lead to the maximum and minimum *DSI* values, respectively. Left: phase shift = 0, which represents the control nonadapted state. Right: phase shift ~π, which represents the adapted state where inhibitory input is shifted by half a cycle due to polarity switch in On-SAC.

(B) DSI as a function of the phase shift between excitatory and inhibitory conductances onto DSGC. DSI values were calculated based on 100 spike trains randomly generated in response to PD and ND stimulation with spiking probability based on DSGC membrane potential. DSI value decreased and became negative for a range of phases around half a cycle shift (i.e., π).

half of the retina, requires cone stimulation, while the loss of the On response, which occurred in both regions of the retina, requires rod saturation.

Several lines of evidence support the idea that a change in rod-cone interactions underlies the polarity switch. First, neither loss of the On response nor gain of the Off response was dependent on depolarization of SACs or inhibitory signaling, ruling out a role for crossover, lateral, and feedback inhibition in the inner retina. Second, prior to adaptation, the On response is mediated in large part by rods, as evidenced by its presence in ventral retina and sensitivity to Cx36. Hence, the loss of the On response is consistent with a loss of rod transduction (Wang et al., 2011).

A more interesting scenario underlies the emergence of the Off response gained after repetitive stimulation. First, it was blocked by L-AP4, indicating that it is mediated by the On pathway. Second, the Off response is dependent on the existence of a high level of tonic glutamate release from On-cone BCs, which appears only after the original On-response has decayed. Furthermore, the magnitude of the Off response is correlated with the duration of the light-induced suppression of glutamate release from On-cone BCs, indicating that it is mediated by the relief of this suppression (Jackman et al., 2009).

How does light stimulation suppress release from On-cone BCs in the adapted circuit? Our hypothesis is that prior to adaptation both rods and cones mediated the On response in dorsal retina (Figure 7), while rods primarily mediate the On response in the ventral retina, though the visual stimulation may also activate the low level of M-opsin in cones in the ventral retina (Wang et al., 2011). After adaptation, rods are unable to hyperpolarize in response to light but, in the dorsal retina, they exhibit the opposite polarity response to light as a result of surround inhibition from cones, leading to a hyperpolarization of the On-cone BCs (Figure 7). One consequence of our model is that stimulating cones in the ventral retina with UV light would reveal a polarity switch in ventral On-SACs. Our preliminary findings support this (Figure S6).

We propose that rods flip their polarity due to negative feedback provided by horizontal cells (Babai and Thoreson, 2009) (Figure 7). In this scenario, cones are hyperpolarized by light, which hyperpolarizes horizontal cells. This leads to a depolarization of saturated rods, which cannot hyperpolarize in response to light. In tiger salamander, Off responses in On-cone BCs have also been observed under conditions of high ambient light (Pang et al., 2012). This Off response was mediated by depolarization of rods and was dependent on AMPA receptor signaling. Indeed, a subsequent study demonstrated that rods may depolarize in response to high light levels via a sign-inverting synapse from cones to horizontal cells to rods (Gao et al., 2013), with a similar phenomenon observed in mice (Babai and Thoreson, 2009). Rod depolarization in response to light stimulation would then propagate through the rod-rod BC circuit, suppressing the release of glutamate from the On-cone BC terminal.

Comparison to Adaptation in Rod-Mediated Light Responses

There are a growing number of examples of adaptation that occur at or presynaptic to On-cone BCs. For example, adaptation to stimulus contrast involves changes in the amount of glutamate released from BCs either because of activation of a conductance in the On-cone BC such as I_h (Manookin and Demb, 2006) or because of differing levels of GABAergic feedback (Nikolaev et al., 2013). In addition, the rod pathway adapts to increasing ambient light levels through changes in the contrast sensitivity via AII cells (Ke et al., 2014) as well as changes in the linearity of retinal ganglion cell integration (Grimes et al., 2014).

Importantly, we showed that signaling through gap junctions amplifies the magnitude of the adapted Off response, implicating changes in signaling in the outer retina as the mechanism for the polarity switch. Though some gap junction blockers have known nonspecific effects (for example, see Vessey et al., 2004), MFA has been demonstrated to functionally block gap junctions without blocking other conductances (Veruki and Hartveit, 2002). Interestingly, gap junctions were found to play a role in reversal of directional preference of On-DSGCs after GABA blockade (Ackert et al., 2009).

Examples of "Switches" in Retinal Circuits

Classically, adaptation has been described as a continuous adjustment to changing statistics of the visual scene. However, more recently, various forms of adaptation in the retina are referred to as "switches," abrupt transitions in circuits as a continuous variable in the environment is changed. First, altering the ambient lights levels can lead to an abrupt change in center-surround properties (Barlow et al., 1957; Farrow et al., 2013). Second, increasing ambient light levels leads to a switch in inner retinal circuits (Grimes et al., 2014), which changes the spatial integration properties of the ganglion cell, referred to by the authors as "repurposing." Finally, PV-5 Off ganglion cells become approach-sensitive in bright light levels and On-Off DSGCs reverse their directional preference following adaptation (Münch et al., 2009; Rivlin-Etzion et al., 2012).

While the segregation between On and Off pathways is one of the most well-known examples of parallel processing in the retina (Wässle, 2004), there is accumulating evidence of interactions between them. Several studies have reported that On-ganglion cells reveal an Off response during blockade of inhibition (Ackert et al., 2009; Nirenberg and Meister, 1997) and Off-ganglion cells display an On response (Farajian et al., 2011; Rentería et al., 2006). On the contrary, the polarity switch we observe is generated by visual stimulation and persists in the absence of normal inhibitory signals. In tiger salamander, an Off-RGC switches its polarity in response to stimulation in the periphery (Geffen et al., 2007). This switch lasts roughly 100 ms and is mediated by a wide-field amacrine cell that releases GABA in response to shifts in the visual scene that occur during a normal saccade. Importantly, the rapid switch does not contradict the anatomy of the cells, as Geffen and colleges classify these switching cells as having On-Off ganglion cell morphology (Geffen et al., 2007).

The physiological implications of the functional switches we observe after adaptation have yet to be determined. An intriguing possible consequence would be that direction-selective cortical neurons inherit their adaptive properties from retinal DSGCs (Kohn and Movshon, 2004; Priebe et al., 2010). This hypothesis is supported by recent findings that there is a disynaptic circuit linking DSGCs to the superficial layers of primary visual cortex (Cruz-Martín et al., 2014). Yet, since our preparation is separated from the pigment epithelium, saturated rods cannot recover and hence our experiment might model a physiological state in which rods are not active. Notably, our results demonstrate that computations performed by anatomically defined neuronal circuits are subject to change after circuit perturbations, emphasizing the necessity of studying both anatomy and physiology while varying the sensory input.

SAC Polarity Switch May Contribute to Reversed Directional Preference of DSGCs

The drifting grating stimulus that induced the polarity switch in this study was chosen because of its ability to reverse the directional preference described in DSGCs (Rivlin-Etzion et al., 2012). However, the cellular and synaptic interactions that link signaling from SACs to DSGCs are complex, with the critical computations occurring at the subcellular level (Taylor and Smith, 2012). Notably, release of GABA is the result of dendritic integration that occurs locally within each SAC process and therefore cannot be assessed with whole-cell recording (Euler et al., 2002).

To explore how a polarity switch could contribute to the reversal of DSGC tuning, we provide a simple model demonstrating how a polarity switch in SACs alters the timing of GABA release relative to the release of glutamate. Based on our results, one interesting prediction is that in ventral retina, where we observed a loss of the On response but no gain of the Off response in SACs, we would expect DSGCs to not reverse their directional preference. A reanalysis of the data from Rivlin-Etzion et al. matched this prediction: DSGCs located in the dorsal retina that were exposed to 200–300 s of the repetitive stimulus (note that not all SACs have switched polarity by this time point; Figure 3) were more likely to reverse their direction preference than DSGCs in ventral retina, which were more likely to remain stably tuned (52% of 41 DSGCs in dorsal retina reversed while 21% of 29 DSGCs in ventral retina reversed; 23% of DSGCs in dorsal retina remained stable while 66% of DSGCs in ventral retina remained stable). Note that this model does not take into account the observation that repetitive stimulation altered the tuning of inhibition, also described in Rivlin-Etzion et al. (2012).

In conclusion, our data represent a dramatic and surprising example of how computations performed by well-defined anatomical circuits depend not only on the wiring diagram between the neurons, but also on the functional connectivity (Bargmann and Marder, 2013) and the visual environment.

EXPERIMENTAL PROCEDURES

More details for each procedure are described in the Supplemental Experimental Procedures.

Animals

All animal procedures were approved by the UC Berkeley Institutional Animal Care and Use Committee and conformed to the NIH Guide for the Care and Use of Laboratory Animals, the Public Health Service Policy, and the SFN Policy on the Use of Animals in Neuroscience Research. Adult mice (P21–P40) were anesthetized with isoflurane and decapitated. Retinas were dissected from enucleated eyes under infrared illumination and oriented as described previously (Wei et al., 2010). Isolated retinas were mounted photoreceptor layer side down and stored in oxygenated Ames media (US Biological) in the dark. Retinas from C57BL/6 mice were used for calcium imaging. For targeted recordings of SACs, we used two mouse lines; On- and Off-SACs were targeted with *mGluR2-GFP* mice (Watanabe et al., 1998) and On-SACs were also targeted with *Chat-cre* mouse (Ivanova et al., 2010) crossed with a reporter line (*tdTomato*, Jackson Laboratory). *Connexin-36* knockout mice (*Cx36* KO) were a generous gift from David Paul at Harvard Medical School (Deans et al., 2002).

Simultaneous Calcium Imaging and Visual Stimulation of DSGCs

Methods are described previously (Briggman and Euler, 2011). Briefly, retinas were electroporated with OGB-1 (Invitrogen) using ten 13–14 V, 10-ms-pulse-width, 1-Hz-pulse-frequency squarewave pulses. The procedure was performed under dim red illumination. Two-photon fluorescence images were obtained with a modified movable objective microscope (MOM) (Sutter Instruments) equipped with through-the-objective UV light stimulation (single LED NC4U134A, peak wavelength 385 nm; Nichia) with the laser tuned to 800 nm. Two kinds of light stimuli were presented while imaging: a series of flashed spots (231 μm diameter) to categorize DSGCs as either On or On-Off and a bar (200 × 350 μm) moving in eight different directions across the field of view at 0.5 mm/s. Each direction was repeated three times.

PSAM-PSEM Neuronal Silencing

AAV2::FLEX-rev::PSAML141F,Y115F:GlyR-IRES-GFP (Magnus et al., 2011) was intravitreally injected into the eyes of P6-8 *ChAT-Cre* mice. To activate PSAM, we perfused retinas with 20 μM PSEM^{89S} for at least 15 min prior to assessing PSAM activation.

Two-Photon Targeted Electrophysiology

Hardware and recording methodology are similar to those in Wei et al. (2010). For conductance measurements, we recorded five sweeps at four different holding potentials (−72 mV, −32 mV, −12 mV, and +8 mV) and averaged across the sweeps. All holding potentials reported here are after correction for the junction potential (−12 mV). For pharmacology experiments, recordings were performed 10 min after Ames media with pharmacological agents at the following concentrations was perfused into the recording chamber: 5 μM L-AP4, 5 μM gabazine, 100 μM MFA, 1 μM strychnine, or 50 μM TPMPA.

Visual Stimulation of SACs

Light spot stimuli (OLED, Emagin) consisted of a 225-μm-diameter white spot presented for 2 s unless otherwise stated. For measuring synaptic currents, the light spot was presented five times at 6 or 8 s intervals at the four different holding potentials listed above. The adapting stimulus consisted of symmetric drifting gratings with 225 μm/cycle, 4 cycle/s, corresponding to 30 deg/s Gratings were first presented for 3 s drifting in eight different directions either four times or eight times in a row; next gratings were presented for 40 s drifting in the nasal direction followed by 40 s drifting in the temporal direction; finally we repeated the presentation of gratings in eight directions. For Figures 4E–4F, bouts of gratings were alternated with light spot stimuli at −72 mV to measure the excitatory current during the adaptation process. For Figures 5F–5G, the duration of the light flash was varied and the light was flashed five times in a row for each duration. To verify that changes in conductance of adapted SACs do not emerge as a result of prolonged whole-cell recordings, we adapted a subset of cells in each experiment before attaching onto them (Table S1).

Statistics

Unless otherwise stated in the results, to compare between control and adapted populations, we ran a Wilcoxon rank-sum test in MATLAB. Significance levels of the difference between median values of the two populations are reported by the p value.

SUPPLEMENTAL INFORMATION

Supplemental Information includes Supplemental Experimental Procedures, six figures, and one table and can be found with this article online at http://dx.doi.org/10.1016/j.neuron.2014.07.037.

AUTHOR CONTRIBUTIONS

A.L.V., M.R.-E., and M.B.F. designed the experiments. A.L.V. and M.R.-E. performed the voltage-clamp recordings and pharmacology from On-SACs. A.L.V. performed the voltage-clamp recordings from Off-SACs and PSAM-expressing SACs. R.B. performed the experiments and analysis of simultaneous visual stimulation and calcium imaging of DSGCs. A.L.V. and R.D.M. performed the fluorescence imaging. R.D.M. performed the viral injections, histology, and resistance measurements from PSAM-expressing SACs. M.R.-E. created the simulation of direction-selective ganglion cell responses. M.R.-E. and A.L.V. did the analysis. C.F. performed vector construction and virus packaging of PSAM. J.G.F. designed the vector and virus. A.L.V., M.R.-E., and M.B.F. wrote the manuscript.

ACKNOWLEDGMENTS

We thank Scott Sternson (Janelia Farms) for the generous gift of PSEM ligand. This work was supported by grants NIH RO1EY019498, RO1EY013528, and P30EY003176. A.L.V. was supported by the National Science Foundation Graduate Research Fellowship Program under Grant No. DGE 1106400; C.F. and J.G.F. were supported by NIH/NEI 1R01EY022975 and the Foundation Fighting Blindness, USA; M. R.-E. was supported by the Human Frontier Science Program Organization and the National Postdoctoral Award Program for Advancing Women in Science; R.D.M was supported by a National Institutes of Health NRSA Trainee appointment on grant number T32 GM 007232.

Accepted: July 18, 2014
Published: August 21, 2014

REFERENCES

Ackert, J.M., Farajian, R., Völgyi, B., and Bloomfield, S.A. (2009). GABA blockade unmasks an OFF response in ON direction selective ganglion cells in the mammalian retina. J. Physiol. *587*, 4481–4495.

Amthor, F.R., Keyser, K.T., and Dmitrieva, N.A. (2002). Effects of the destruction of starburst-cholinergic amacrine cells by the toxin AF64A on rabbit retinal directional selectivity. Vis. Neurosci. *19*, 495–509.

Applebury, M.L., Antoch, M.P., Baxter, L.C., Chun, L.L., Falk, J.D., Farhangfar, F., Kage, K., Krzystolik, M.G., Lyass, L.A., and Robbins, J.T. (2000). The murine cone photoreceptor: a single cone type expresses both S and M opsins with retinal spatial patterning. Neuron *27*, 513–523.

Babai, N., and Thoreson, W.B. (2009). Horizontal cell feedback regulates calcium currents and intracellular calcium levels in rod photoreceptors of salamander and mouse retina. J. Physiol. *587*, 2353–2364.

Bargmann, C.I., and Marder, E. (2013). From the connectome to brain function. Nat. Methods *10*, 483–490.

Barlow, H., Fitzhugh, R., and Kuffler, S. (1957). Change of organization in the receptive fields of the cat's retina during dark adaptation. J. Physiol. *137*, 338–354.

Borghuis, B.G., Marvin, J.S., Looger, L.L., and Demb, J.B. (2013). Two-photon imaging of nonlinear glutamate release dynamics at bipolar cell synapses in the mouse retina. J. Neurosci. *33*, 10972–10985.

Breuninger, T., Puller, C., Haverkamp, S., and Euler, T. (2011). Chromatic bipolar cell pathways in the mouse retina. J. Neurosci. *31*, 6504–6517.

Briggman, K.L., and Euler, T. (2011). Bulk electroporation and population calcium imaging in the adult mammalian retina. J. Neurophysiol. *105*, 2601–2609.

Briggman, K.L., Helmstaedter, M., and Denk, W. (2011). Wiring specificity in the direction-selectivity circuit of the retina. Nature *471*, 183–188.

Calderone, J.B., and Jacobs, G.H. (1995). Regional variations in the relative sensitivity to UV light in the mouse retina. Vis. Neurosci. *12*, 463–468.

Cruz-Martín, A., El-Danaf, R.N., Osakada, F., Sriram, B., Dhande, O.S., Nguyen, P.L., Callaway, E.M., Ghosh, A., and Huberman, A.D. (2014). A dedicated circuit links direction-selective retinal ganglion cells to the primary visual cortex. Nature *507*, 358–361.

Dalkara, D., Byrne, L.C., Lee, T., Hoffmann, N.V., Schaffer, D.V., and Flannery, J.G. (2012). Enhanced gene delivery to the neonatal retina through systemic administration of tyrosine-mutated AAV9. Gene Ther. *19*, 176–181.

Dalkara, D., Byrne, L.C., Klimczak, R.R., Visel, M., Yin, L., Merigan, W.H., Flannery, J.G., and Schaffer, D.V. (2013). In vivo-directed evolution of a new adeno-associated virus for therapeutic outer retinal gene delivery from the vitreous. Sci. Transl. Med. *5*, 189ra76.

Dedek, K., Schultz, K., Pieper, M., Dirks, P., Maxeiner, S., Willecke, K., Weiler, R., and Janssen-Bienhold, U. (2006). Localization of heterotypic gap junctions composed of connexin45 and connexin36 in the rod pathway of the mouse retina. Eur. J. Neurosci. *24*, 1675–1686.

Deans, M.R., Volgyi, B., Goodenough, D.A., Bloomfield, S.A., and Paul, D.L. (2002). Connexin36 is essential for transmission of rod-mediated visual signals in the mammalian retina. Neuron *36*, 703–712.

Ekesten, B., and Gouras, P. (2005). Cone and rod inputs to murine retinal ganglion cells: evidence of cone opsin specific channels. Vis. Neurosci. *22*, 893–903.

Enroth-Cugell, C., and Shapley, R.M. (1973). Adaptation and dynamics of cat retinal ganglion cells. J. Physiol. *233*, 271–309.

Euler, T., Detwiler, P.B., and Denk, W. (2002). Directionally selective calcium signals in dendrites of starburst amacrine cells. Nature *418*, 845–852.

Farajian, R., Pan, F., Akopian, A., Völgyi, B., and Bloomfield, S.A. (2011). Masked excitatory crosstalk between the ON and OFF visual pathways in the mammalian retina. J. Physiol. *589*, 4473–4489.

Farrow, K., Teixeira, M., Szikra, T., Viney, T.J., Balint, K., Yonehara, K., and Roska, B. (2013). Ambient illumination toggles a neuronal circuit switch in the retina and visual perception at cone threshold. Neuron *78*, 325–338.

Fried, S.I., Münch, T.A., and Werblin, F.S. (2002). Mechanisms and circuitry underlying directional selectivity in the retina. Nature *420*, 411–414.

Gao, F., Pang, J.-J., and Wu, S.M. (2013). Sign-preserving and sign-inverting synaptic interactions between rod and cone photoreceptors in the dark-adapted retina. J. Physiol. *591*, 5711–5726.

Geffen, M.N., de Vries, S.E.J., and Meister, M. (2007). Retinal ganglion cells can rapidly change polarity from Off to On. PLoS Biol. *5*, e65.

Grimes, W.N., Schwartz, G.W., and Rieke, F. (2014). The synaptic and circuit mechanisms underlying a change in spatial encoding in the retina. Neuron *82*, 460–473.

Helmstaedter, M., Briggman, K.L., Turaga, S.C., Jain, V., Seung, H.S., and Denk, W. (2013). Connectomic reconstruction of the inner plexiform layer in the mouse retina. Nature *500*, 168–174.

Ivanova, E., Hwang, G.S., and Pan, Z.H. (2010). Characterization of transgenic mouse lines expressing Cre recombinase in the retina. Neuroscience *165*, 233–243.

Jackman, S.L., Choi, S.-Y., Thoreson, W.B., Rabl, K., Bartoletti, T.M., and Kramer, R.H. (2009). Role of the synaptic ribbon in transmitting the cone light response. Nat. Neurosci. *12*, 303–310.

Ke, J.-B., Wang, Y.V., Borghuis, B.G., Cembrowski, M.S., Riecke, H., Kath, W.L., Demb, J.B., and Singer, J.H. (2014). Adaptation to background light enables contrast coding at rod bipolar cell synapses. Neuron *81*, 388–401.

Kohn, A., and Movshon, J.A. (2004). Adaptation changes the direction tuning of macaque MT neurons. Nat. Neurosci. *7*, 764–772.

Lee, S., Kim, K., and Zhou, Z.J. (2010). Role of ACh-GABA cotransmission in detecting image motion and motion direction. Neuron *68*, 1159–1172.

Magnus, C.J., Lee, P.H., Atasoy, D., Su, H.H., Looger, L.L., and Sternson, S.M. (2011). Chemical and genetic engineering of selective ion channel-ligand interactions. Science *333*, 1292–1296.

Manookin, M.B., and Demb, J.B. (2006). Presynaptic mechanism for slow contrast adaptation in mammalian retinal ganglion cells. Neuron *50*, 453–464.

Masland, R.H. (2012). The neuronal organization of the retina. Neuron *76*, 266–280.

Münch, T.A., da Silveira, R.A., Siegert, S., Viney, T.J., Awatramani, G.B., and Roska, B. (2009). Approach sensitivity in the retina processed by a multifunctional neural circuit. Nat. Neurosci. *12*, 1308–1316.

Nikolaev, A., Leung, K.-M., Odermatt, B., and Lagnado, L. (2013). Synaptic mechanisms of adaptation and sensitization in the retina. Nat. Neurosci. *16*, 934–941.

Nirenberg, S., and Meister, M. (1997). The light response of retinal ganglion cells is truncated by a displaced amacrine circuit. Neuron *18*, 637–650.

Olveczky, B.P., Baccus, S.A., and Meister, M. (2007). Retinal adaptation to object motion. Neuron *56*, 689–700.

Pang, J.-J., Gao, F., and Wu, S.M. (2012). Ionotropic glutamate receptors mediate OFF responses in light-adapted ON bipolar cells. Vision Res. *68*, 48–58.

Park, S.J.H., Kim, I.-J., Looger, L.L., Demb, J.B., and Borghuis, B.G. (2014). Excitatory synaptic inputs to mouse on-off direction-selective retinal ganglion cells lack direction tuning. J. Neurosci. *34*, 3976–3981.

Priebe, N.J., Lampl, I., and Ferster, D. (2010). Mechanisms of direction selectivity in cat primary visual cortex as revealed by visual adaptation. J. Neurophysiol. *104*, 2615–2623.

Rentería, R.C., Tian, N., Cang, J., Nakanishi, S., Stryker, M.P., and Copenhagen, D.R. (2006). Intrinsic ON responses of the retinal OFF pathway are suppressed by the ON pathway. J. Neurosci. *26*, 11857–11869.

Rieke, F., and Rudd, M.E. (2009). The challenges natural images pose for visual adaptation. Neuron *64*, 605–616.

Rivlin-Etzion, M., Wei, W., and Feller, M.B. (2012). Visual stimulation reverses the directional preference of direction-selective retinal ganglion cells. Neuron *76*, 518–525.

Sagdullaev, B.T., McCall, M.A., and Lukasiewicz, P.D. (2006). Presynaptic inhibition modulates spillover, creating distinct dynamic response ranges of sensory output. Neuron *50*, 923–935.

Slaughter, M.M., and Miller, R.F. (1981). 2-amino-4-phosphonobutyric acid: a new pharmacological tool for retina research. Science *211*, 182–185.

Taylor, W.R., and Smith, R.G. (2012). The role of starburst amacrine cells in visual signal processing. Vis. Neurosci. *29*, 73–81.

Taylor, W.R., and Vaney, D.I. (2002). Diverse synaptic mechanisms generate direction selectivity in the rabbit retina. J. Neurosci. *22*, 7712–7720.

Vaney, D.I., Sivyer, B., and Taylor, W.R. (2012). Direction selectivity in the retina: symmetry and asymmetry in structure and function. Nat. Rev. Neurosci. *13*, 194–208.

Veruki, M.L., and Hartveit, E. (2002). Electrical synapses mediate signal transmission in the rod pathway of the mammalian retina. J. Neurosci. *22*, 10558–10566.

Vessey, J.P., Lalonde, M.R., Mizan, H.A., Welch, N.C., Kelly, M.E., and Barnes, S. (2004). Carbenoxolone inhibition of voltage-gated Ca channels and synaptic transmission in the retina. J. Neurophysiol. *92*, 1252–1256.

Wang, Y.V., Weick, M., and Demb, J.B. (2011). Spectral and temporal sensitivity of cone-mediated responses in mouse retinal ganglion cells. J. Neurosci. *31*, 7670–7681.

Wässle, H. (2004). Parallel processing in the mammalian retina. Nat. Rev. Neurosci. *5*, 747–757.

Watanabe, D., Inokawa, H., Hashimoto, K., Suzuki, N., Kano, M., Shigemoto, R., Hirano, T., Toyama, K., Kaneko, S., Yokoi, M., et al. (1998). Ablation of cerebellar Golgi cells disrupts synaptic integration involving GABA inhibition and NMDA receptor activation in motor coordination. Cell *95*, 17–27.

Wei, W., and Feller, M.B. (2011). Organization and development of direction-selective circuits in the retina. Trends Neurosci. *34*, 638–645.

Wei, W., Elstrott, J., and Feller, M.B. (2010). Two-photon targeted recording of GFP-expressing neurons for light responses and live-cell imaging in the mouse retina. Nat. Protoc. *5*, 1347–1352.

Wei, W., Hamby, A.M., Zhou, K., and Feller, M.B. (2011). Development of asymmetric inhibition underlying direction selectivity in the retina. Nature *469*, 402–406.

Werblin, F.S. (2010). Six different roles for crossover inhibition in the retina: correcting the nonlinearities of synaptic transmission. Vis. Neurosci. *27*, 1–8.

Yonehara, K., Farrow, K., Ghanem, A., Hillier, D., Balint, K., Teixeira, M., Jüttner, J., Noda, M., Neve, R.L., Conzelmann, K.-K., and Roska, B. (2013). The first stage of cardinal direction selectivity is localized to the dendrites of retinal ganglion cells. Neuron *79*, 1078–1085.

Yoshida, K., Watanabe, D., Ishikane, H., Tachibana, M., Pastan, I., and Nakanishi, S. (2001). A key role of starburst amacrine cells in originating retinal directional selectivity and optokinetic eye movement. Neuron *30*, 771–780.